Electronic Supplementary Material (ESI) for Dalton Transactions.

Supporting Information for

Triphenylamine-Containing Imine-linked Porous Organic Network for Luminescent Detection and Adsorption of Cr(VI) in Water

Man Wang,[a] Han-Shu Li,[a] Xin Ding,[a] Lizan Jiang,[a] Pengyan Wu,*[a] Ruiting Zheng,[a] Guoyue Bao,[a] Guoliang Liu*[b] and Jian Wang*[a]

[a]School of Chemistry and Materials Science & Jiangsu Key Laboratory of Green Synthetic Chemistry for Functional Materials, Jiangsu Normal University, Xuzhou 221116, China.

[b]State Key Laboratory of Materials-Oriented Chemical Engineering, College of Chemical Engineering, Nanjing Tech University, Nanjing 211816, China.

E-mail: wpyan@jsnu.edu.cn; glliu@njtech.edu.cn; wjian@jsnu.edu.cn

1. Materials and Methods.

Reagents and chemicals: All reagents and solvents were of AR grade and used without further purification unless otherwise noted. 1,2-Diphenylethylenediamine (DPEA) and tris(4-formylphenyl)amine (TFPA) were purchased from Alfa Aesar. Anion salts ($K_2Cr_2O_7$, K_2CrO_4, K_2CO_3, $KHCO_3$, K_2S, K_2SO_4, KNO_3, KF, KCl, KBr, KI, K_3PO_4, $KMnO_4$, K_2HPO_4, KH_2PO_4 and $K_4P_2O_7$) were purchased from J&K Scientific. Stock solution (2×10^{-2} M) of the anion salts were prepared in water for further experiments.

Instruments and spectroscopic measurements: The elemental analyses of C, H and N were performed on a Vario EL III elemental analyzer. Solid-state nuclear magnetic resonance (NMR) data were collected on a Bruker Avance 400 MHz NMR spectrometer (DRX400) with cross-polarization magic-angle spinning (CP/MAS). X-Ray powder diffraction (XRD) patterns of the PON-1 was recorded on a Rigaku D/max-2400 X−ray powder diffractometer (Japan) using Cu-*K*α (λ = 1.5405 Å) radiation. X-ray photoelectron spectroscopy (XPS) experiments were performed with a PHI QUANTUM2000 surface analysis instrument. The morphologies of the prepared samples were recorded by a Field Emission Scanning Electron Microscopy (SEM) of Hitachi SU8010. Samples were treated *via* Pt sputtering for 90 s before observation. Transmission electron microscopy (TEM) was conducted on a FEI-Tecnai G2 transmission electron microscope. FT−IR spectra were recorded as KBr pellets on JASCO FT/IR−430. Thermogravimetric analysis (TGA) was carried out at a ramp rate of 5 °C/min in a nitrogen flow with a Mettler-Toledo TGA/SDTA851 instrument. Fluorescence spectra of the solution were obtained using the FP6500 spectrometer (JASCO). Both excitation and emission slit widths were

2.5 nm. Fluorescence measurements were carried out in a 1 cm quartzcuvette with stirring the suspension of PON-1.

Synthesis of PON-1: A 10 mL Pyrex tube was charged with 1,2-Diphenylethylenediamine (DPEA) (15.9 mg, 0.075 mmol), tris(4-formylphenyl)amine (TFPA) (16.5 mg, 0.05 mmol), mesitylene/dioxane (1:1 v/v, 3 mL), and aqueous acetic acid (6 M, 0.5 mL). The mixture was sonicated for 15 min to get a homogeneous dispersion. The tube was then flash frozen at 77 K with a liquid N_2 bath and degassed by three freeze-pump-thaw cycles, sealed under vacuum, and heated at 120 °C for 3 days. The brown precipitate was collected by centrifugation and washed with anhydrous acetone, anhydrous tetrahydrofuran, and anhydrous ethanol, separately. The collected powder was then activated by solvent exchange with anhydrous methanol 3 times and air dried to give a pale brown powder with 80% isolated yield and a molecular formula of $(C_{84}H_{66}N_8)_n$ (% calcd/found: C 84.96/84.85, H 5.60/5.56, N 9.44/9.45).

Table S1. The proposed model was geometry-optimized using the MS Forcite molecular dynamics module (universal force fields, Ewald summations) to obtain the optimized lattice parameters, see bellow:

	PON-1	
Empirical formula	$C_{84}H_{66}N_8$	$C_{162}H_{126}N_{16}$
Formula wt	1187.4768	2296.8417
Stacking method	slipped-AA	slipped-AB
Crystal System	Triclinic	Triclinic
Space Group	*P*1	*P*1
a (Å)	29.1225	29.1225
b (Å)	28.7659	28.7659
c (Å)	3.6000	7.2000
α (°)	90.00	90.00
β (°)	90.00	90.00
γ (°)	120.00	120.00

Table S2. Atomic coordinates of the AA-stacking mode of PON-1.

Atom site label	Atom site fract x	Atom site fract y	Atom site fract z	Atom site label	Atom site fract x	Atom site fract y	Atom site fract z
C1	1.48579	-1.50434	-0.44284	C24	1.36301	-1.37558	-0.67509
C2	1.51671	-1.44244	-0.55717	C25	1.40095	-1.39160	-0.66053
N3	1.51723	-1.52948	-0.54376	C26	1.53856	-1.64078	-0.59609
C4	1.42647	-1.53663	-0.55412	C27	1.57751	-1.65562	-0.59962
N5	1.48527	-1.41730	-0.45625	C28	1.62927	-1.62180	-0.45820
C6	1.57603	-1.41015	-0.44589	C29	1.63949	-1.57120	-0.32491
C7	1.39076	-1.52043	-0.42350	C30	1.60155	-1.55518	-0.33948
C8	1.33655	-1.55020	-0.50105	N31	1.33241	-1.30855	-0.55176
C9	1.31579	-1.59913	-0.68539	C32	1.27542	-1.34979	-0.54631
C10	1.34947	-1.61767	-0.79948	C33	1.34838	-1.25090	-0.55429
C11	1.40406	-1.58673	-0.73750	N34	1.67009	-1.63823	-0.44824
C12	1.61174	-1.42635	-0.57651	C35	1.72708	-1.59699	-0.45368
C13	1.66595	-1.39658	-0.49896	C36	1.65412	-1.69588	-0.44571
C14	1.68671	-1.34765	-0.31462	C37	1.60512	-1.73564	-0.29722
C15	1.65303	-1.32911	-0.20054	C38	1.58781	-1.79036	-0.32658
C16	1.59845	-1.36005	-0.26252	C39	1.62014	-1.80777	-0.48786
C17	1.49353	-1.37072	-0.56516	C40	1.67006	-1.76942	-0.61755
C18	1.45186	-1.35664	-0.52877	C41	1.68639	-1.71485	-0.59991
C19	1.50897	-1.57606	-0.43485	C42	1.76645	-1.60658	-0.30347
C20	1.55064	-1.59014	-0.47124	C43	1.82047	-1.56925	-0.33274
C21	1.46394	-1.30600	-0.40391	C44	1.83753	-1.51930	-0.49687

C22	1.42499	-1.29116	-0.40038	C45	1.79955	-1.50773	-0.63405
C23	1.37323	-1.32498	-0.54180	C46	1.74572	-1.54604	-0.61823
C47	1.23605	-1.34020	-0.69653	C73	0.92817	-1.66156	-0.73896
C48	1.18203	-1.37753	-0.66726	C74	0.97760	-1.63896	-0.56809
C49	1.16497	-1.42748	-0.50313	C75	1.00558	-1.58411	-0.48654
C50	1.20295	-1.43905	-0.36595	C76	1.46734	-0.90738	-0.77062
C51	1.25678	-1.40074	-0.38177	C77	1.44174	-0.87812	-0.83978
C52	1.39738	-1.21114	-0.70277	C78	1.38898	-0.89880	-0.73729
C53	1.41469	-1.15642	-0.67342	C79	1.36174	-0.94885	-0.56660
C54	1.38236	-1.13901	-0.51214	C80	1.38778	-0.97735	-0.48555
C55	1.33244	-1.17736	-0.38244	C81	1.56103	-1.98958	-0.41591
C56	1.31611	-1.23193	-0.40009	C82	2.01700	-1.39674	-0.41536
C57	1.40232	-1.08203	-0.42598	C83	1.53517	-2.03940	-0.22937
N58	1.44306	-1.04323	-0.59460	C84	1.56076	-2.06866	-0.16022
C59	1.47042	-0.98737	-0.46062	C85	1.61352	-2.04798	-0.26270
C60	1.10862	-1.46457	-0.42086	C86	1.64076	-1.99793	-0.43340
N61	1.07037	-1.46226	-0.59198	C87	1.61472	-1.96943	-0.51445
C62	1.01510	-1.49059	-0.46025	C88	2.06617	-1.37299	-0.22833
C63	1.89388	-1.48221	-0.57913	C89	2.09491	-1.31783	-0.15869
N64	1.93213	-1.48452	-0.40802	C90	2.07433	-1.28522	-0.26103
C65	1.98740	-1.45619	-0.53974	C91	2.02490	-1.30782	-0.43191
C66	1.60018	-1.86475	-0.57401	C92	1.99692	-1.36267	-0.51345
N67	1.55944	-1.90355	-0.40539	H93	1.48355	-1.50719	-0.14598
C68	1.53208	-1.95941	-0.53938	H94	1.51895	-1.43958	-0.85403

C69	0.98550	-1.55004	-0.58463	H95	1.40348	-1.48647	-0.24146
C70	1.44147	-0.95720	-0.58408	H96	1.31027	-1.53647	-0.40161
C71	0.93633	-1.57378	-0.77166	H97	1.27361	-1.62287	-0.73704
C72	0.90759	-1.62895	-0.84130	H98	1.33337	-1.65594	-0.93997
H99	1.42776	-1.60325	-0.82978	H125	1.19085	-1.47707	-0.23002
H100	1.59902	-1.46031	-0.75855	H126	1.28307	-1.41193	-0.25968
H101	1.69223	-1.41032	-0.59840	H127	1.42447	-1.22116	-0.82561
H102	1.72889	-1.32391	-0.26297	H128	1.45424	-1.12794	-0.76349
H103	1.66914	-1.29084	-0.06004	H129	1.30670	-1.16502	-0.25212
H104	1.57474	-1.34353	-0.17024	H130	1.27792	-1.25839	-0.28908
H105	1.52917	-1.34316	-0.71005	H131	1.38538	-1.07375	-0.18629
H106	1.47333	-1.60362	-0.28997	H132	1.46645	-0.98920	-0.16289
H107	1.50352	-1.27793	-0.30618	H133	1.10025	-1.49009	-0.18146
H108	1.43734	-1.25204	-0.29709	H134	1.01672	-1.49288	-0.16251
H109	1.32560	-1.40416	-0.78825	H135	1.90225	-1.45669	-0.81853
H110	1.39116	-1.43048	-0.77082	H136	1.98578	-1.45390	-0.83749
H111	1.49898	-1.66885	-0.69383	H137	1.61712	-1.87303	-0.81370
H112	1.56516	-1.69474	-0.70291	H138	1.53605	-1.95758	-0.83711
H113	1.67690	-1.54262	-0.21175	H139	0.91996	-1.55021	-0.87204
H114	1.61134	-1.51630	-0.22919	H140	0.86966	-1.64635	-0.98097
H115	1.57803	-1.72562	-0.17439	H141	0.90613	-1.70418	-0.79635
H116	1.54826	-1.81884	-0.23651	H142	0.99367	-1.66425	-0.48832
H117	1.69580	-1.78176	-0.74788	H143	1.04203	-1.56960	-0.33561
H118	1.72458	-1.68839	-0.71091	H144	1.50700	-0.89090	-0.87055

H119	1.75667	-1.64387	-0.17832	H145	1.46259	-0.83969	-0.97902
H120	1.84870	-1.58046	-0.23873	H146	1.36903	-0.87636	-0.79427
H121	1.81165	-1.46971	-0.76998	H147	1.32072	-0.96500	-0.48654
H122	1.71943	-1.53485	-0.74032	H148	1.36561	-1.01423	-0.33450
H123	1.24583	-1.30291	-0.82168	H149	1.49550	-2.05588	-0.12945
H124	1.15380	-1.36632	-0.76126	H150	1.53991	-2.10709	-0.02097
H151	1.63347	-2.07042	-0.20572	H155	2.13284	-1.30043	-0.01902
H152	1.68178	-1.98179	-0.51345	H156	2.09637	-1.24260	-0.20364
H153	1.63690	-1.93255	-0.66550	H157	2.00883	-1.28253	-0.51167
H154	2.08254	-1.39657	-0.12795	H158	1.96047	-1.37718	-0.66438

Figure S1. Powder X-ray diffraction (PXRD) patterns of as-synthesized PON-1 and simulated PON-1 in different stacking models.

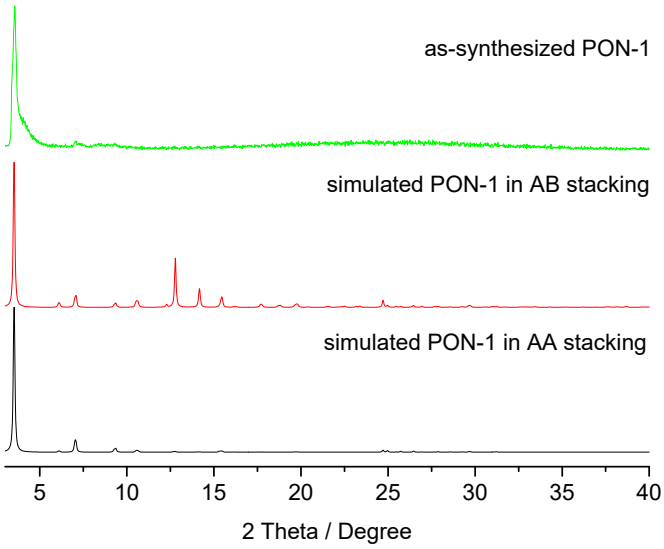

Figure S2. ^{13}C NMR spectra of PON-1.

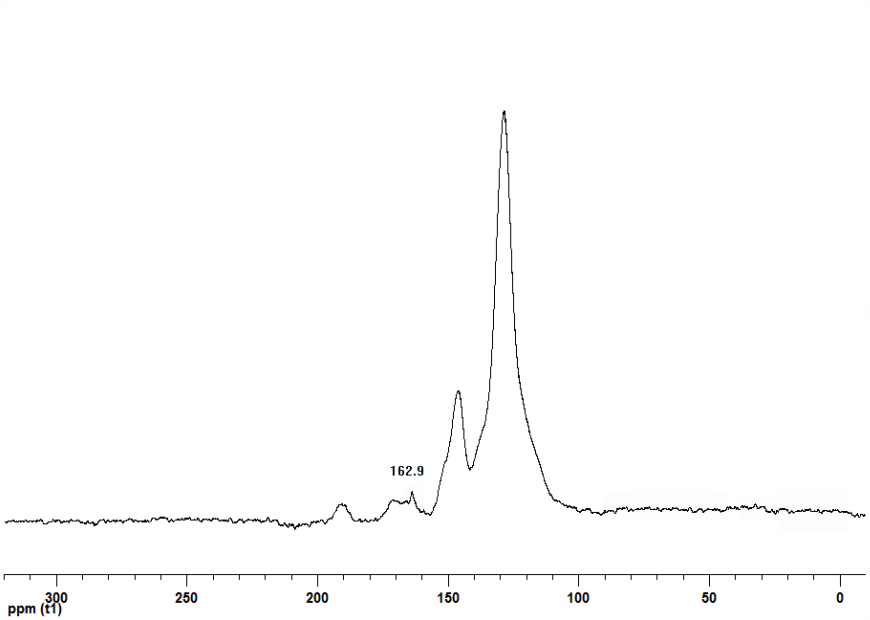

Figure S3. TGA traces of PON-1 ranging from room temperature to 600 °C.

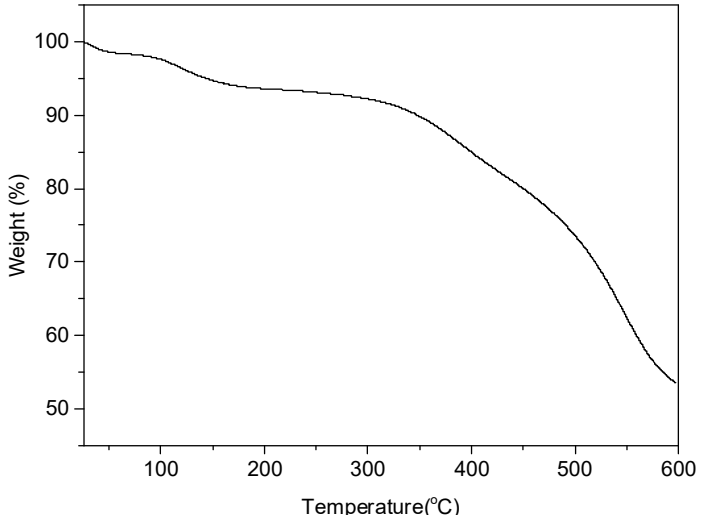

Figure S4. N_2 physisorption isotherms of PON-1.

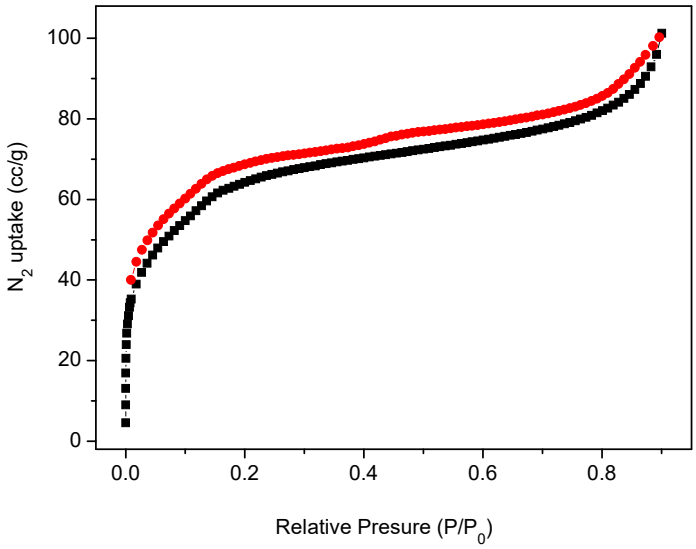

Figure S5. Pore size distribution of PON-1.

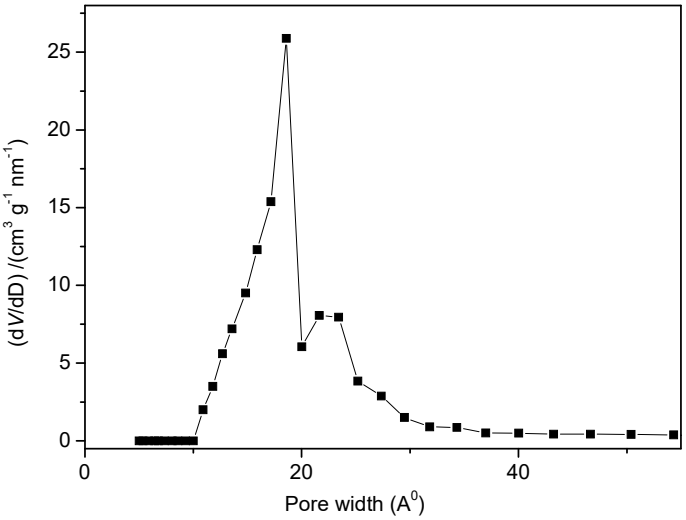

Figure S6. pH-dependent fluorescence of PON-1 in aqueous with the pH ranging from 4.0 to 11.0.

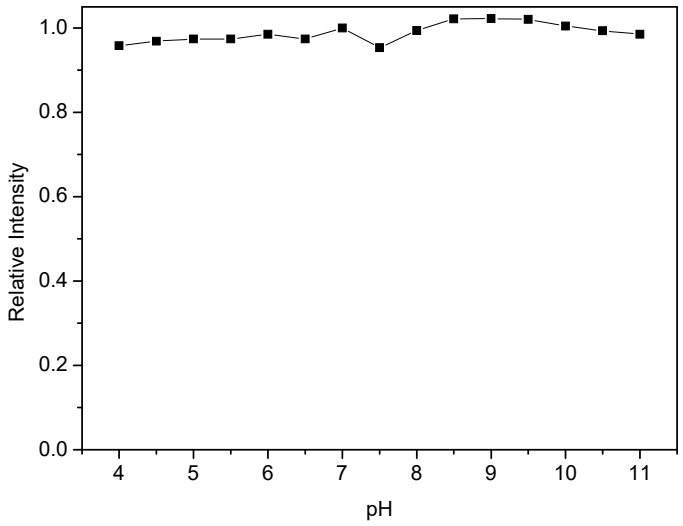

Figure S7. Families of various fluorescence spectra of PON-1 in water solution upon the addition of 2.98 mM of different selected anions.

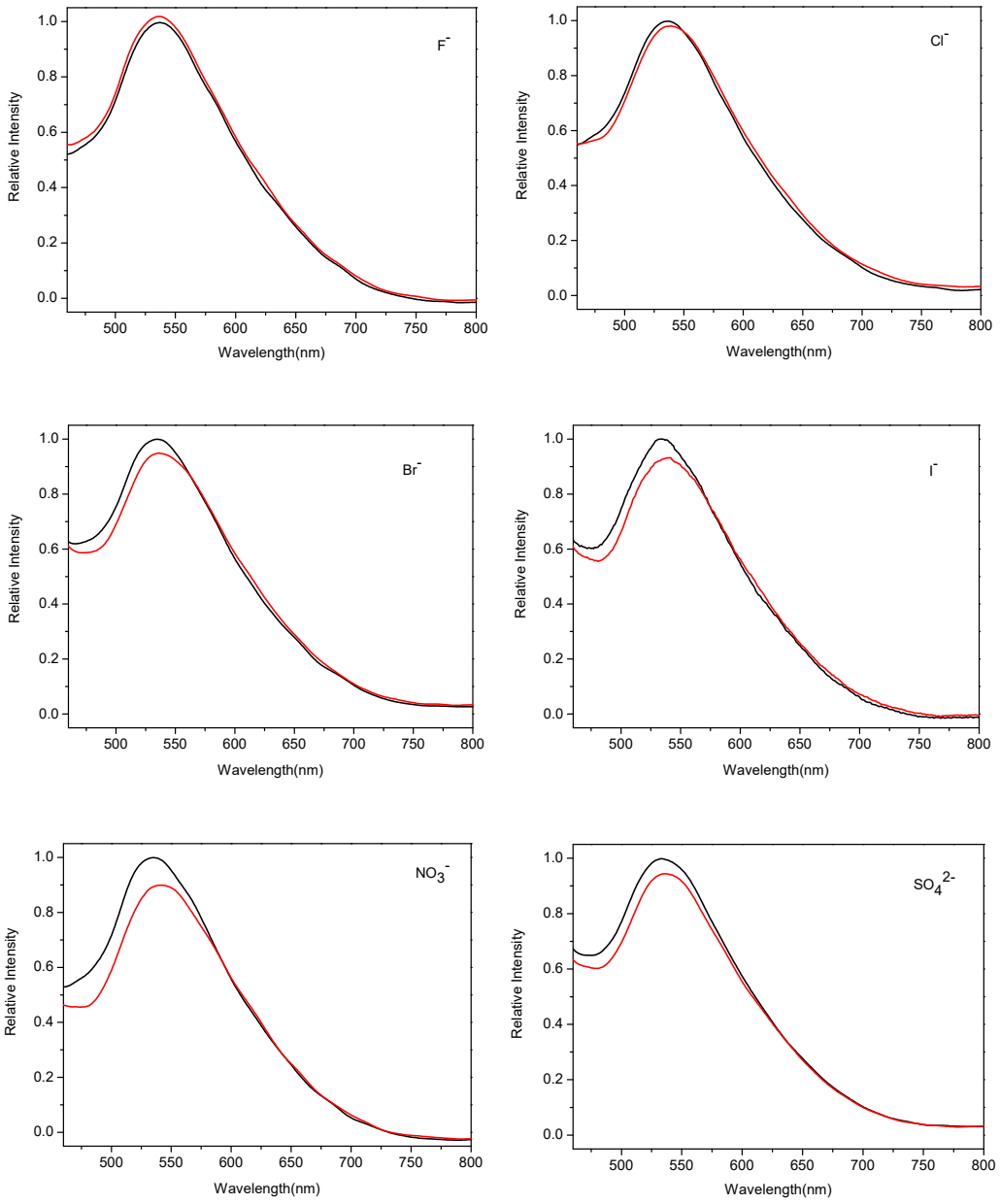

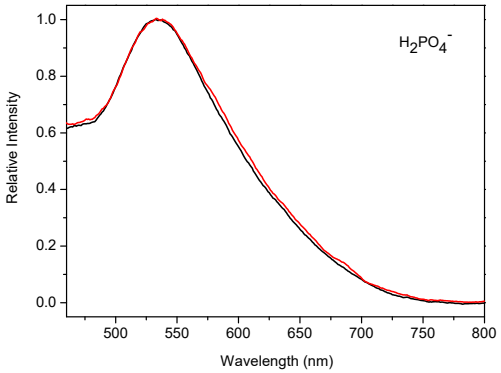
$H_2PO_4^-$
Relative Intensity
Wavelength (nm)

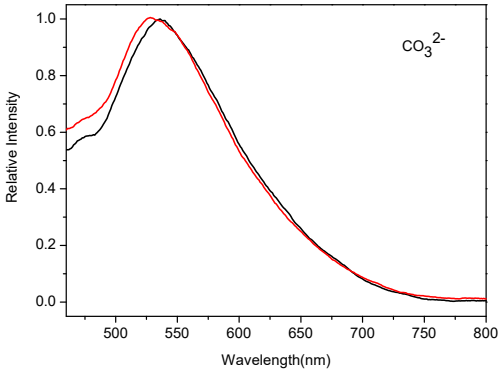
CO_3^{2-}
Relative Intensity
Wavelength(nm)

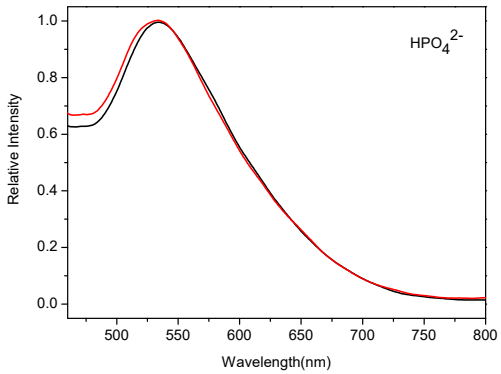
HPO_4^{2-}
Relative Intensity
Wavelength(nm)

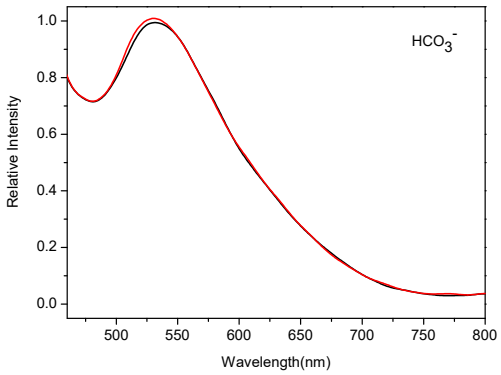
HCO_3^-
Relative Intensity
Wavelength(nm)

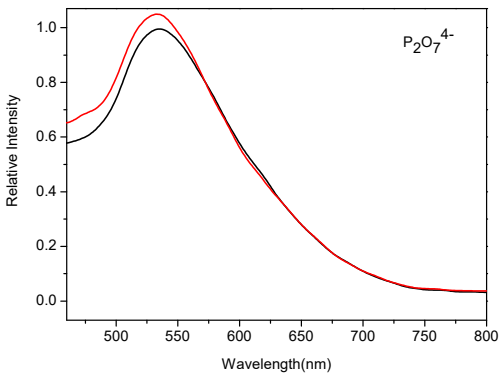
$P_2O_7^{4-}$
Relative Intensity
Wavelength(nm)

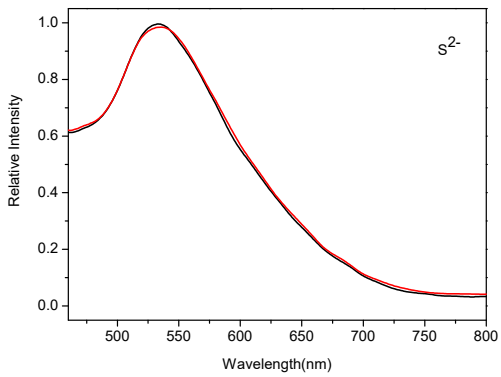
S^{2-}
Relative Intensity
Wavelength(nm)

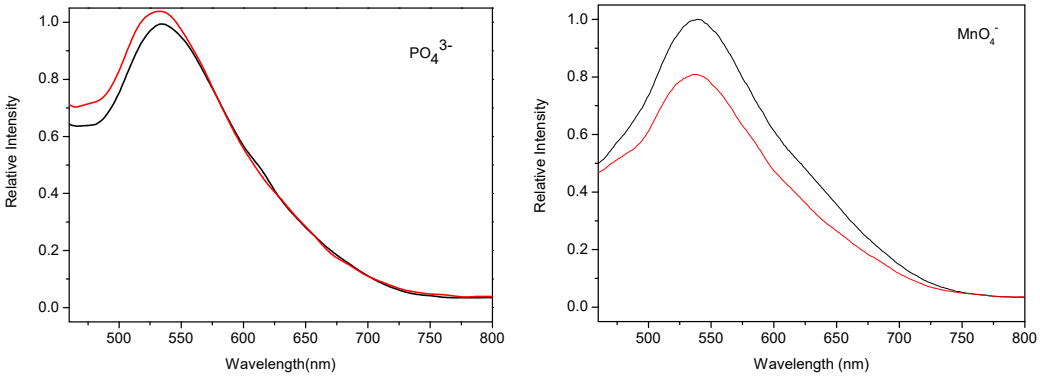

Figure S8. Fluorescence spectra of PON-1 as a function of the CrO_4^{2-} concentration (from 0.0 to 2.98 mM) in an aqueous solution with λ_{ex} = 420 nm.

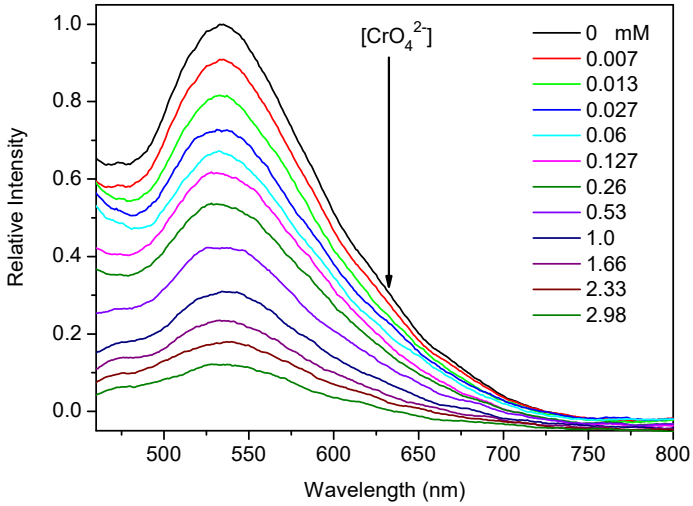

Figure S9. The Stern−Volmer plot of PON-1 quenched by $Cr_2O_7^{2-}$ (top) and CrO_4^{2-} (bottom), where I_0 and I are the fluorescence intensity before and after $Cr_2O_7^{2-}$ or CrO_4^{2-} incorporation, respectively.

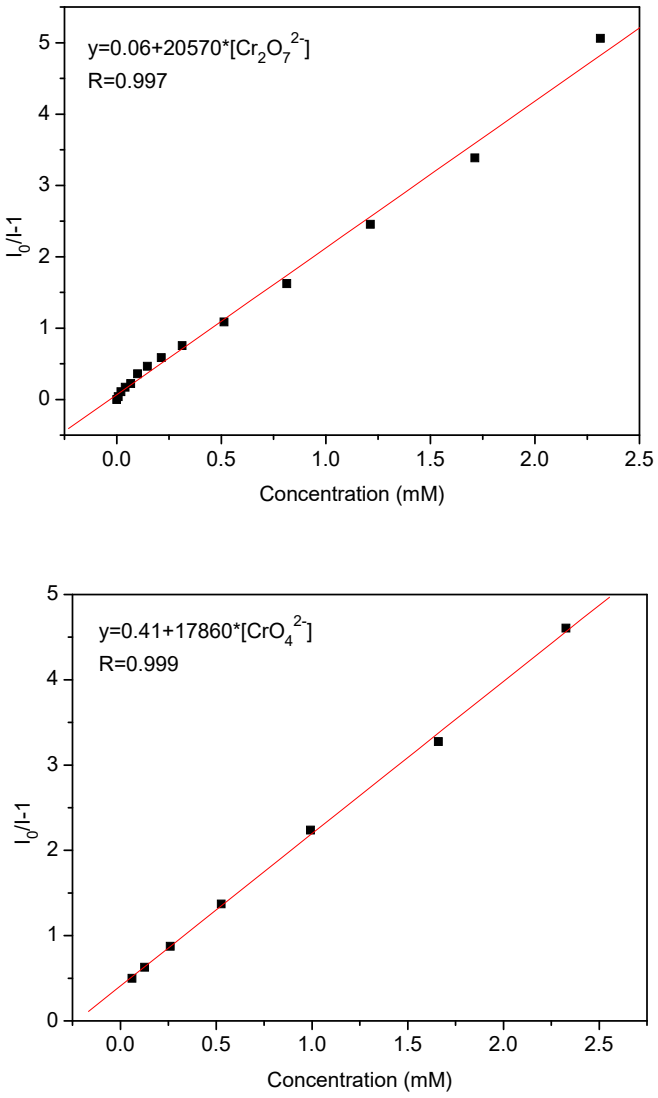

Figure S10. Plot of the relative fluorescence intensity of PON-1 as the concentration of $Cr_2O_7^{2-}$ (left) and CrO_4^{2-} (right).

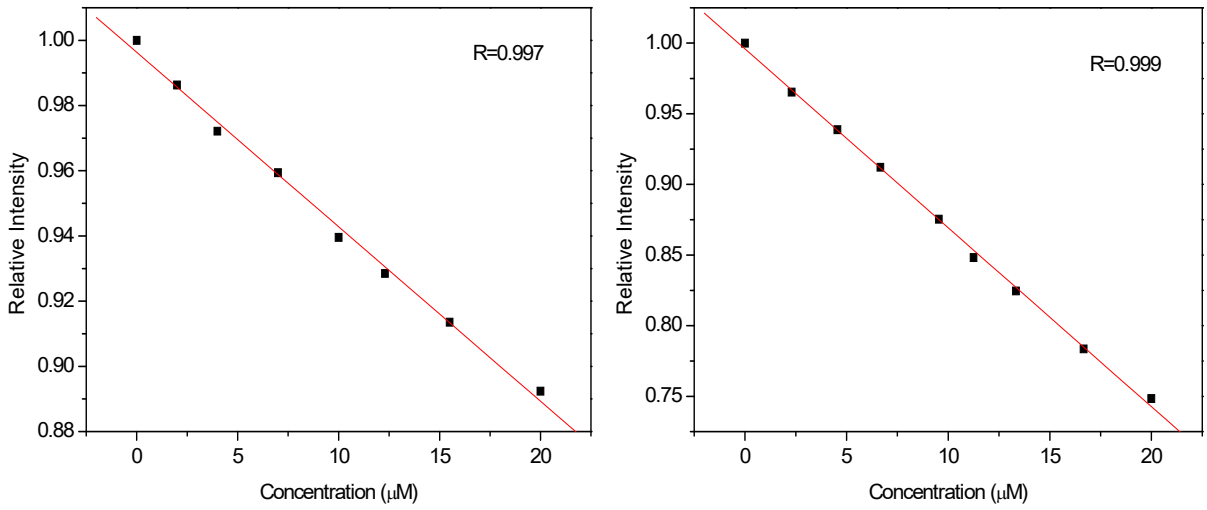

To determine the S/N ratio, the emission intensity of PON-1 without Cr(VI) was measured for 10 times and the standard deviation of blank measurements was determined. The detection limit is then calculated with the following equation:

$$LOD = K \times \delta / S$$

Where δ is the standard deviation of blank measurements, S is the slope between intensity versus sample concentration.

$\delta = \sqrt{\frac{\sum(F_0 - F_i)^2}{N-1}} = 0.331$ (N =10); K = 3

The LOD for $Cr_2O_7^{2-}$: Linear Equation: $y = 2.84 \times 10^6 \times x + 0.996$; R = 0.997

$$LOD = K \times \delta / S = 3.5 \times 10^{-7}\ M$$

The LOD for CrO_4^{2-}: Linear Equation: $y = 2.48 \times 10^6 \times x + 0.983$; R = 0.999

$$LOD = K \times \delta / S = 4.0 \times 10^{-7}\ M$$

Figure S11. The fluorescence intensity of PON-1 with varying CrO_4^{2-} concentrations.

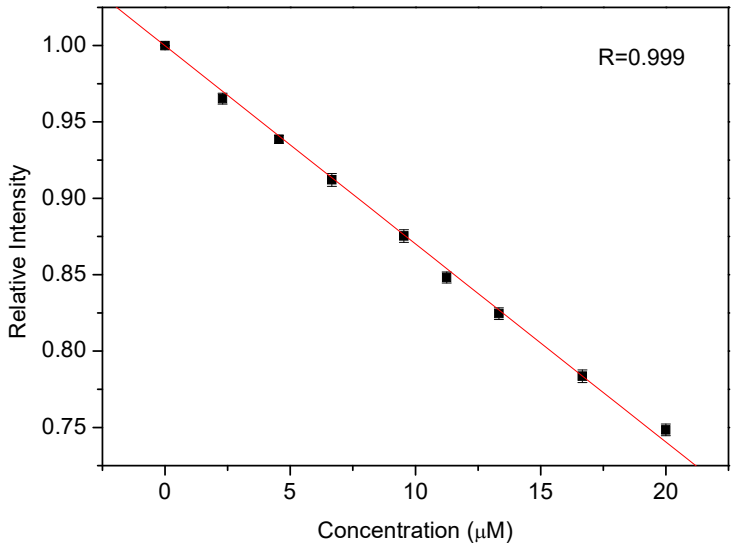

Figure S12. Fluorescence spectra of PON-1 with gradual addition of different concentrations of $Cr_2O_7^{2-}$ (top) or CrO_4^{2-} (bottom) in HEPES buffer solutions.

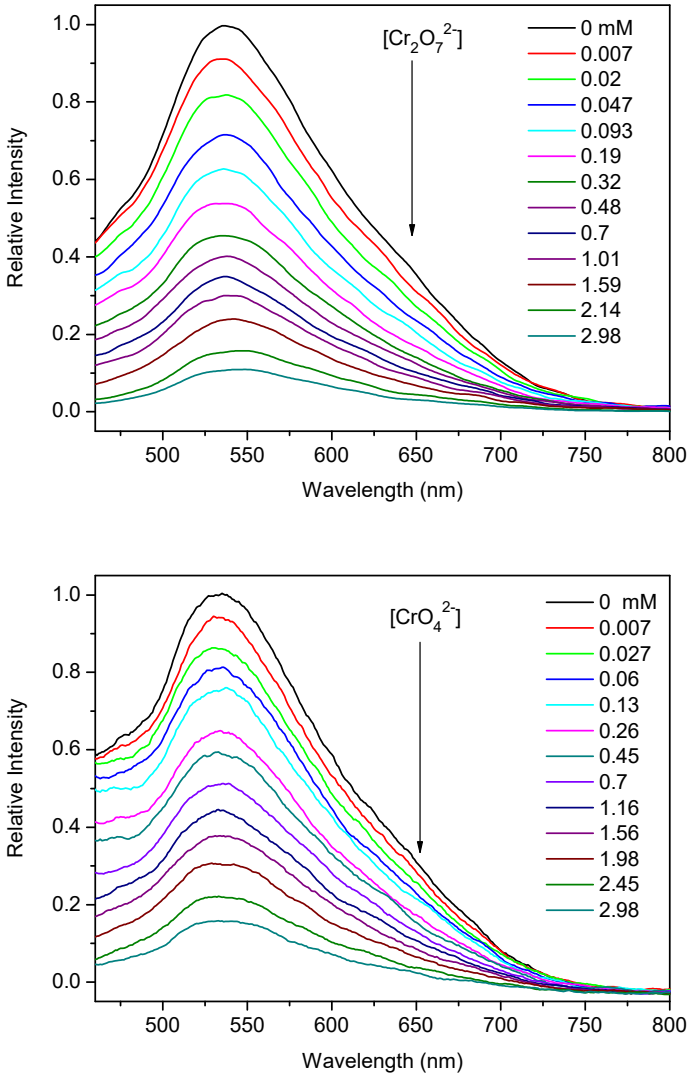

Figure S13. The Stern−Volmer plot of PON-1 quenched by $Cr_2O_7^{2-}$ (top) and CrO_4^{2-} (bottom) in HEPES buffer solutions, where I_0 and I are the fluorescence intensity before and after $Cr_2O_7^{2-}$ or CrO_4^{2-} incorporation, respectively.

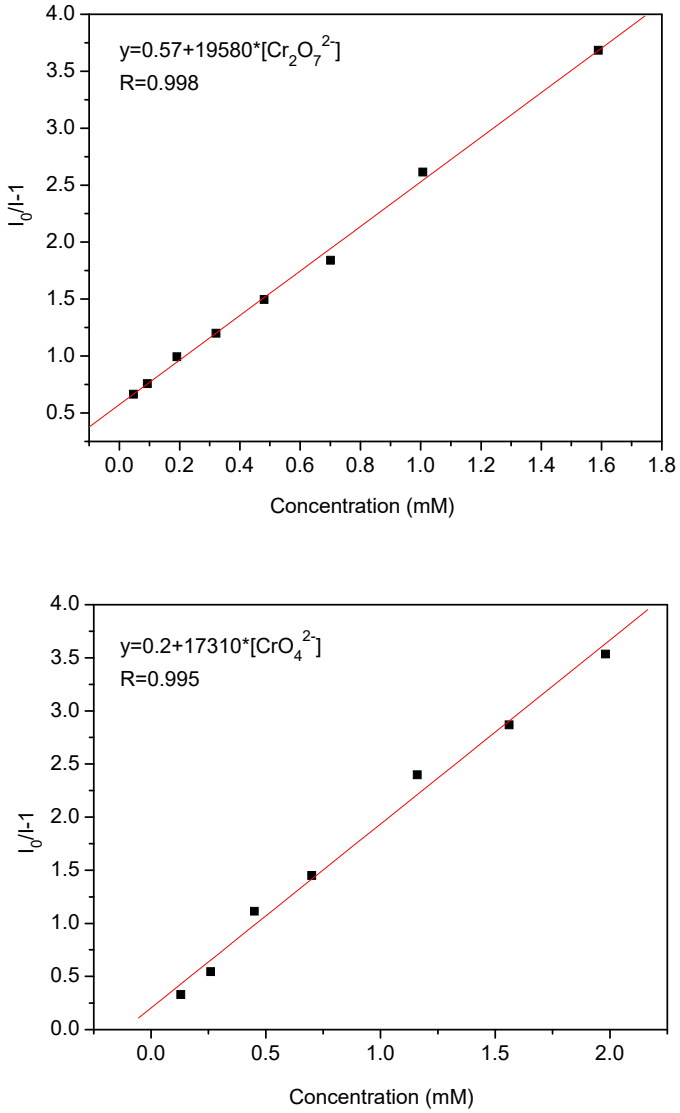

Figure S14. Effect of initial $Cr_2O_7^{2-}$ (top) and CrO_4^{2-} (bottom) concentration on the adsorption capacity of PON-1.

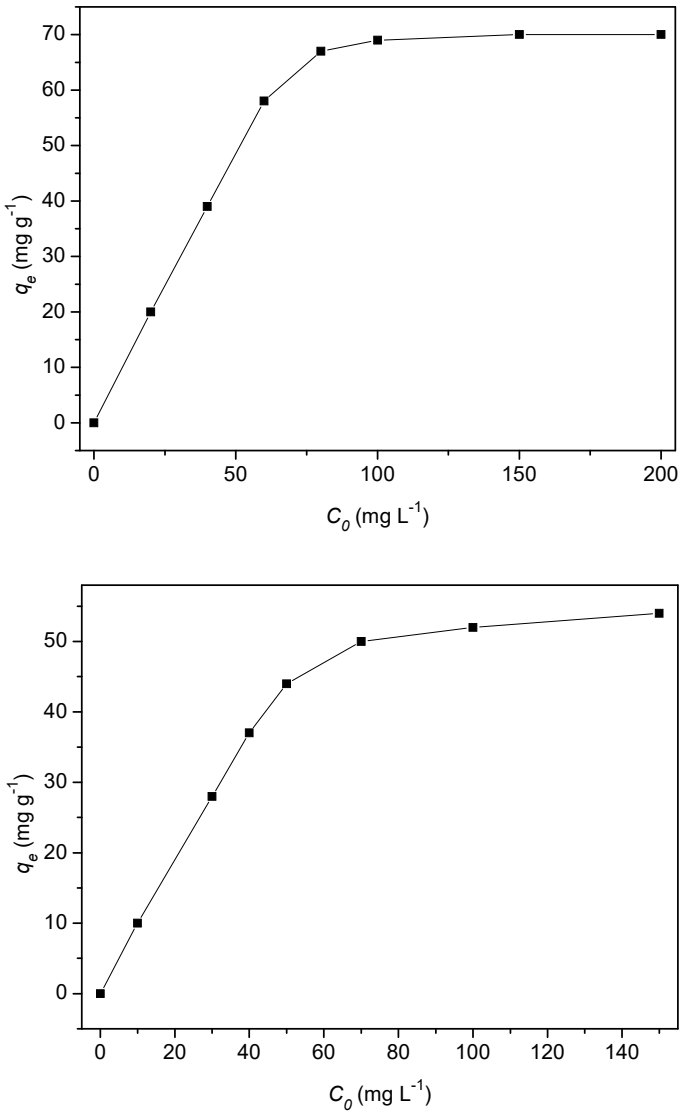

Figure S15. The adsorption capacity of PON-1 for $Cr_2O_7^{2-}$ (top) and CrO_4^{2-} (bottom) with varying $Cr_2O_7^{2-}$ and CrO_4^{2-} concentrations.

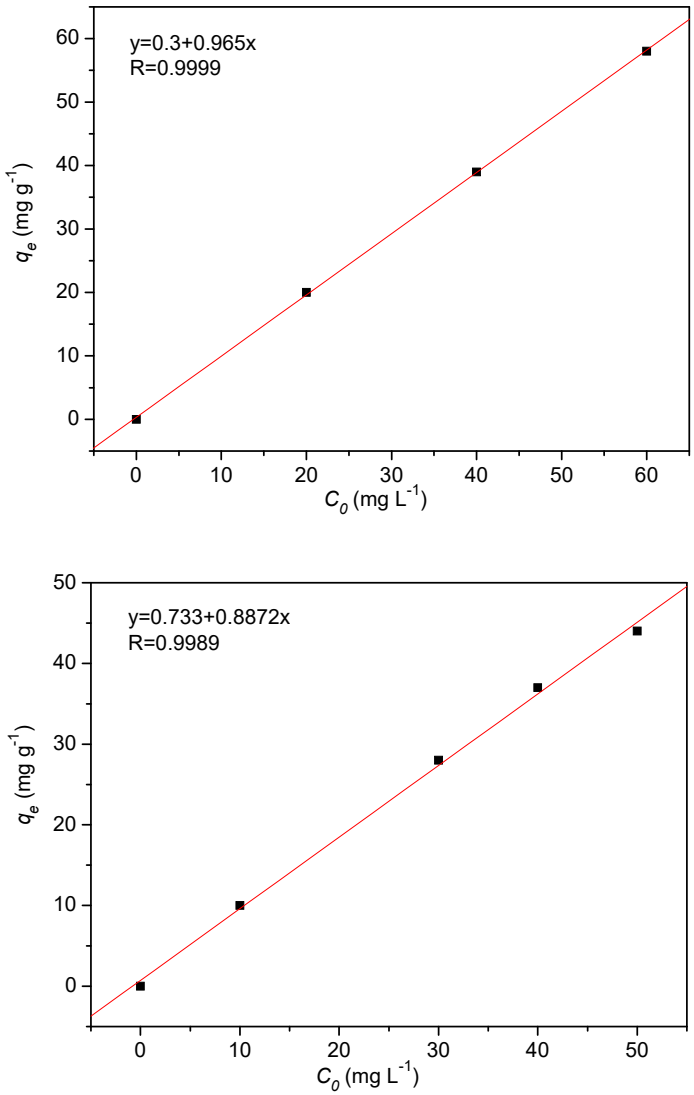

Table S3. Comparison of the detective sensitivity in various porous polymer for Cr(VI).

No.	LMOF/LPON	Analyte	K_{sv} (M^{-1})	Detection limit	Ref.
1	$[Ni_2(\mu_2\text{-OH})(azdc)(tpim)](NO_3)\cdot 6DMA\cdot 6MeOH$	$Cr_2O_7^{2-}$ CrO_4^{2-}	1.31×10^4 7.9×10^3	0.9 *ppm* 0.29 *ppm*	S1
2	$\{[Zn(PA^{-2})(4,4'\text{-bpy})](H_2O)\}_n$	$Cr_2O_7^{2-}$	4.8×10^3	4.12 μM	S2
3	$[Cd_{1.5}(L_1)_2(bpy)(NO_3)]\cdot 2DMF\cdot 2H_2O$	$Cr_2O_7^{2-}$ CrO_4^{2-}	5.42×10^4 1.73×10^4	320 *ppm* 280 *ppm*	S3
4	$[Cd(4\text{-tkpvb})(5\text{-}tert\text{-BIPA})]_n$	$Cr_2O_7^{2-}$ CrO_4^{2-}	4.68×10^4 2.50×10^4	8.00×10^{-8} M 1.20×10^{-7} M	S4
5	$\{[Zn(IPA)(L_8)]\}_n$ $\{[Zn(IPA)(L_8)]\}_n$	$Cr_2O_7^{2-}$ CrO_4^{2-} $Cr_2O_7^{2-}$ CrO_4^{2-}	1.37×10^3 1.00×10^3 1.37×10^3 1.00×10^3	12.02 μM 18.33 μM 12.02 μM 18.33 μM	S5
6	Zr-MOF-3 Hf-MOF-3	$Cr_2O_7^{2-}$ $Cr_2O_7^{2-}$	6.37×10^5 4.51×10^5	0.013 μM 0.019 μM	S6
7	$\{[Eu(L_9)(HCOO)]\cdot H_2O\}_n$	$Cr_2O_7^{2-}$ CrO_4^{2-}	3.1×10^4 2.0×10^4	2×10^{-9} M 1×10^{-9} M	S7
8	$\{[Cd_2(bptc)(4,4'\text{-bipy})(H_2O)_2]\cdot 4H_2O\}_n$ $\{[Cd_2(bptc)(2,2'\text{-bipy})_2(H_2O)_2]\}_n$ $\{[Cd_2(bptc)(phen)_2]\cdot 4H_2O\}_n$	$Cr_2O_7^{2-}$ CrO_4^{2-} $Cr_2O_7^{2-}$ CrO_4^{2} $Cr_2O_7^{2-}$ CrO_4^{2}	9.34×10^3 5.38×10^3 1.17×10^4 7.95×10^3 2.09×10^3 1.09×10^3	1.36×10^{-5} M 1.6×10^{-5} M 7.38 μM 7.79 μM 5.89×10^{-5} M 1.06×10^{-4} M	S8
9	$[Eu_2(tpbpc)_4\cdot CO_3\cdot 4H_2O]\cdot DMF$	$Cr_2O_7^{2-}$ CrO_4^{2-}	1.04×10^4 4.85×10^3	1.07 *ppm* 0.33 *ppm*	S9
10	$\{[Zn_3(mtrb)_3(btc)_2]\cdot 3H_2O\}_n$	$Cr_2O_7^{2-}$ CrO_4^{2-}	4.62×10^3 2.77×10^3	2.83 μM 4.52 μM	S10
11	$[Ag(CIP^-)]$	$Cr_2O_7^{2-}$ CrO_4^{2-}	6.3×10^4 2×10^4	1.4×10^{-7} M 4.5×10^{-7} M	S11
12	ZR-1	$Cr_2O_7^{2-}$ CrO_4^{2-}	8.94×10^3 1.11×10^4	50 μM —	S12
13	$[Cd(L_4)_2(H_2O)_2]_n$	$Cr_2O_7^{2-}$ CrO_4^{2-}	5.1×10^4 1.1×10^4	3.41×10^{-5} M 1.75×10^{-4} M	S13
14	$[Zn(opda)(bib)]_n$	$Cr_2O_7^{2-}$	1.54×10^7	2.99×10^{-7} M	S14
15	$[Cd(2\text{-bpeb})_{0.5}(CNA)(H_2O)]_n$ $[Cd(2\text{-bpeb})_{0.5}(NDC)]_n$ $[Zn(2\text{-bpeb})(BDC)]_n$	$Cr_2O_7^{2-}$ $Cr_2O_7^{2-}$ $Cr_2O_7^{2-}$	7.61×10^3 3.10×10^3 1.88×10^3	3.67×10^{-4} M 9.20×10^{-4} M 1.44×10^{-3} M	S15
16	TMU-41	$Cr_2O_7^{2-}$ CrO_4^{2-}	1.00×10^6 6.10×10^5	0.02 μM 0.03 μM	S16
17	$[Zn(L_6)(H_2O)]\cdot H_2O$	$Cr_2O_7^{2-}$ CrO_4^{2-}	2.07×10^4 1.02×10^4	3.53 μM 4.80 μM	S17
18	$[Pb(C_{20}H_{10}N_2O_4S)(DMF)]$ $[Mn_4(C_{20}H_{10}N_2O_4S)_2(HCOO)_4(DEF)_2]$	$Cr_2O_7^{2-}$ CrO_4^{2-} $Cr_2O_7^{2-}$ CrO_4^{2-}	1.12×10^5 1.7×10^4 1.21×10^5 1.56×10^4	153 *ppb* 441 *ppb* 71 *ppb* 303 *ppb*	S18
19	$[Zn(L_{11})_{0.5}(bidpe)]_n$	$Cr_2O_7^{2-}$ CrO_4^{2-}	6.20×10^4 5.54×10^4	4.80×10^{-7} 5.40×10^{-7}	S19
20	$\{[Zn(ATA)(L_2)]\cdot H_2O\}_n$	$Cr_2O_7^{2-}$ CrO_4^{2-}	2.62×10^3 1.48×10^3	4.30×10^{-7} 2.50×10^{-7}	S20
21	$[Zn_2(TPOM)(NH_2\text{-BDC})_2]\cdot 4H_2O$	$Cr_2O_7^{2-}$ CrO_4^{2-}	7.59×10^3 4.45×10^3	3.9 μM 4.8 μM	S21

22	$[\{Zn_2(5N_3\text{-IPA})_2(4,4'\text{-azp})_2\}(H_2O)_8]_\infty$	$Cr_2O_7^{2-}$ CrO_4^{2-}	5.87×10^4 2.1×10^4	4 nM 11 nM	S22
23	$[Tb_{0.2}Y_{0.8}(FDA)(Ox)_{0.5}(H_2O)_2]\cdot H_2O$	CrO_4^{2-}	3.46×10^6	1.1 nM	S23
24	$\{[(CH_3)_2NH_2]_2[Eu_4(FDA)_7(DMF)_2]\cdot 0.5DMF\}_n$ $\{[(CH_3)_2NH_2]_2[Tb_4(FDA)_7(DMF)_2]\cdot 0.5DMF\}_n$	$Cr_2O_7^{2-}$ CrO_4^{2-} $Cr_2O_7^{2-}$ CrO_4^{2-}	1.25×10^4 3.56×10^3 1.46×10^4 4.35×10^3	1.14×10^{-4} M 1.12×10^{-4} M 7.42×10^{-5} M 1.27×10^{-4} M	S24
25	$[Eu_7(mtb)_5(H_2O)_{16}]\cdot NO_3\cdot 8DMA\cdot 18H_2O$	CrO_4^{2-}	3.3×10^4	0.56 *ppb*	S25
26	$\{[Cd_2(L_{10})_2(adi)_2]\cdot 5H_2O\}_\infty$ $\{[Cd(L_{10})(glu)]\cdot 3H_2O\}_\infty$ $\{[Cd(L_{10})(sub)]\cdot 3H_2O\cdot DMA\}_\infty$	$Cr_2O_7^{2-}$ $Cr_2O_7^{2-}$ $Cr_2O_7^{2}$	8.626×10^3 1.027×10^4 7.790×10^3	1.126 *ppm* 1.196 *ppm* 0.831 *ppm*	S26
27	$[Eu(ipbp)_2(H_2O)_3]\cdot Br\cdot 6H_2O$	$Cr_2O_7^{2-}$ CrO_4^{2}	8.98×10^3 7.08×10^3	5.16 μM 5.82 μM	S27
28	$Zr_6O_4(OH)_7(H_2O)_3(BTBA)_3$	$Cr_2O_7^{2-}$	1.57×10^4	1.5 μM	S28
29	$\{[Cd_2(L_{11})(DCTP)_2]\cdot 3.75H_2O\}_n$	$Cr_2O_7^{2-}$	9.56×10^3	1.99×10^{-5} M	S29
30	$\{[(CH_3)_2NH_2]_2[Zn_5(TDA)_4(TZ)_4]\cdot 4DMF\}_n$	$Cr_2O_7^{2-}$ CrO_4^{2}	6.67×10^3 5.48×10^3	7.48 μM 14.46 μM	S30
31	$\{[Cd(L_7)(BPDC)]\cdot 2H_2O\}_n$ $\{[Cd(L_7)(SDBA)(H_2O)]\cdot 0.5H_2O\}_n$	$Cr_2O_7^{2-}$ $Cr_2O_7^{2-}$	6.40×10^3 4.97×10^3	3.76×10^{-5} M 4.86×10^{-5} M	S31
32	$\{[Eu_3(bcbp)_3(NO_3)_7]\cdot NO_3\cdot ClO_4\}_n$	$Cr_2O_7^{2-}$	1.40×10^4	5.6 μM	S32
33	$\{[Eu_2(L_3)_{1.5}(H_2O)_2EtOH]\cdot DMF\}_n$	$Cr_2O_7^{2-}$	1.5×10^3	10^{-5} M	S33
34	RhB@9-1-MOF-253-NH_2	$Cr_2O_7^{2-}$ CrO_4^{2}	— —	0.863 μM 0.789 μM	S34
35	COF-TT	$Cr_2O_7^{2-}$ CrO_4^{2}	1.4×10^4 1.4×10^4	3.43×10^{-4} M 3.43×10^{-4} M	S35
36	POP-Im1	$Cr_2O_7^{2-}$	n/a	n/a	S36
37	PON-1	$Cr_2O_7^{2-}$ CrO_4^{2}	2.0×10^4 1.78×10^4	0.35 μM 0.4 μM	This work

References:

S1. R. Goswami, N. Seal, S. R. Dash, A. Tyagi and S. Neogi, *ACS Appl. Mater. Interfaces*, 2019, 11, 40134-40150.

S2. H. Kaur, S. Sinha, V. Krishnan and R. R. Koner, *Ind. Eng. Chem. Res.*, 2020, 59, 8538-8550.

S3. M. Singh, S. Senthilkumar, S. Rajput and S. Neogi, *Inorg. Chem.*, 2020, 59, 3012-3025.

S4. W. J. Gong, R. Yao, H. X. Li, Z. G. Ren, J. G. Zhang and J. P. Lang, *Dalton Trans.*, 2017, 46, 16861-16871.

S5. B. Parmar, Y. Rachuri, K. K. Bisht, R. Laiya and E. Suresh, *Inorg. Chem*., 2017, 56, 2627-2638.

S6. K. Wu, J. Zheng, Y.-L. Huang, D. Luo, Y. Y. Li, W. Lu and D. Li, *J. Mater. Chem. C*, 2020, 8, 16974-16983.

S7. Y. Liu, J. Ma, C. Xu, Y. Yang, M. Xia, H. Jiang and W. Liu, *Dalton Trans.*, 2018, 47, 13543-13549.

S8. Y. Lin, X. Zhang, W. Chen, W. Shi and P. Cheng, *Inorg. Chem.*, 2017, 56, 11768-11778.

S9. J. Liu, G. Ji, J. Xiao and Z. Liu, *Inorg. Chem.*, 2017, 56, 4197-4205.

S10. Y.-Q. Zhang, V. A. Blatov, T.-R. Zheng, C.-H. Yang, L.-L. Qian, K. Li, B.-L. Li and B. Wu, *Dalton Trans.*, 2018, 47, 6189-6198.

S11. D.-D. Feng, Y.-D. Zhao, X.-Q. Wang, D.-D. Fang, J. Tang, L.-M. Fan and J. Yang, *Dalton Trans.*, 2019, 48, 10892-10900.

S12. T.-T. Han, J. Yang, Y.-Y. Liu and J.-F. Ma, *Microporous Mesoporous Mater.*, 2016, 228, 275-288.

S13. Y.-T. Yan, F. Cao, W.-Y. Zhang, S.-S. Zhang, F. Zhang and Y.-Y. Wang, *New J. Chem.*, 2018, 42, 9865-9875.

S14. C. G. Xu, C. F. Bi, Z. Zhu, R. Luo, X. Zhang, D. M. Zhang, C. B. Fan, L. S. Cui and Y. H. Fan, *Crystengcomm*, 2019, 21, 2333-2344.

S15. X.-D. Zhang, Y. Zhao, K. Chen, Y.-F. Jiang and W.-Y. Sun, *Chem.-Asian J.*, 2019, 14, 3620-3626.

S16. N. Abdollahi and A. Morsali, *Anal. Chim. Acta.*, 2019, 1064, 119-125.

S17. X.-Y. Guo, F. Zhao, J.-J. Liu, Z.-L. Liu and Y.-Q. Wang, *J. Mater. Chem. A,* 2017, 5, 20035-20043.

S18. A. K. Jana and S. Natarajan, *ChemPlusChem*, 2017, 82, 1153-1163.

S19. C. G. Xu, C. F. Bi, Z. Zhu, R. Luo, X. Zhang, D. M. Zhang, C. B. Fan, L. S. Cui and Y. H. Fan, *Crystengcomm*, 2019, 21, 2333-2344.

S20. B. Parmar, Y. Rachuri, K. K. Bisht and E. Suresh, *Inorg. Chem.*, 2017, 56, 10939-10949.

S21. R. Lv, J. Wang, Y. Zhang, H. Li, L. Yang, S. Liao, W. Gu and X. Liu, *J. Mater. Chem. A*, 2016, 4, 15494-15500.

S22. S. Mukherjee, S. Ganguly, D. Samanta and D. Das, *ACS Sustainable Chem. Eng.*, 2020, 8, 1195-1206.

S23. D. K. Singha, P. Majee, S. Hui, S. K. Mondal and P. Mahata, *Dalton Trans.*, 2020, 49, 829-840.

S24. J.-Y. Zou, L. Li, S.-Y. You, Y.-W. Liu, H.-M. Cui, J.-Z. Cui and S.-W. Zhang, *Dalton Trans.*, 2018, 47, 15694-15702.

S25. W. Liu, Y. Wang, Z. Bai, Y. Li, Y. Wang, L. Chen, L. Xu, J. Diwu, Z. Chai and S. Wang, *ACS Appl. Mater. Interfaces*, 2017, 9, 16448-16457.

S26. Y.-Q. Chen, Y. Tian, S.-L. Yao, J. Zhang, R.-Y. Feng, Y.-J. Bian and S.-J. Liu, *Chem.-Asian J.*, 2019, 14, 4420-4428.

S27. C. Zhang, L. Sun, Y. Yan, H. Shi, B. Wang, Z. Liang and J. Li, *J. Mater. Chem. C*, 2017, 5, 8999-9004.

S28. T. He, Y.-Z. Zhang, X.-J. Kong, J. Yu, X.-L. Lv, Y. Wu, Z.-J. Guo and J.-R. Li, *ACS Appl. Mater. Interfaces*, 2018, 10, 16650-16659.

S29. Y.-S. Shi, D. Liu, L. Fu, Y.-H. Li and G.-Y. Dong, *CrystEngComm*, 2020, 22, 4079-4093.

S30. J.-Y. Zou, L. Li, S.-Y. You, H.-M. Cui, Y.-W. Liu, K.-H. Chen, Y.-H. Chen, J.-Z. Cui and S.-W. Zhang, *Dyes Pigm.*, 2018, 159, 429-438.

S31. S. Chen, Z. Shi, L. Qin, H. Jia and H. Zheng, *Cryst. Growth Des.*, 2017, 17, 67-72.

S32. Z. Li, W. Cai, X. Yang, A. Zhou, Y. Zhu, H. Wang, X. Zhou, K. Xiong, Q. Zhang and Y. Gai, *Cryst. Growth Des.*, 2020, 20, 3466-3473.

S33. W. Liu, X. Huang, C. Xu, C. Chen, L. Yang, W. Dou, W. Chen, H. Yang and W. Liu, *Chem.-Eur. J.*, 2016, 22, 18769-18776.

S34. Y. Jin, H. Lu and B. Yan, *Dyes Pigments*, 2021, 194, 109588.

S35. M. Li, Z. H. Cui, S. R. Pang, L. K. Meng, D. X. Ma, Y. Li, Z. Shi and S. H. Feng, *J. Mater. Chem. C*, 2019, 7, 11919-11925.

S36. Y. Su, Y. Wang, X. Li, X. Li and R. Wang, *ACS Appl. Mater. Interfaces*, 2016, 8, 18904.